

Compositional Deformations, Absorption Spectroscopy, and Low-Temperature X-Ray Diffraction of $\text{Sr}_{1-x}\text{Ba}_x\text{Bi}_2\text{B}_2\text{O}_7$ Solid Solutions

A. P. Shablinskii^{a,*}, R. S. Bubnova^a, A. V. Povolotskii^b, and S. K. Filatov^b

^a *Grebenschikov Institute of Silicate Chemistry, Russian Academy of Sciences, St. Petersburg, 199034 Russia*

^b *St. Petersburg State University, St. Petersburg, 199034 Russia*

*e-mail: shablinskii.andrey@mail.ru

Received November 3, 2023; revised November 9, 2023; accepted November 24, 2023

Abstract—Thermal expansion of $\text{SrBi}_2\text{B}_2\text{O}_7$ borate was investigated by in situ powder X-ray diffraction in the temperature range from -175 to 25°C . Compositional deformations of $\text{Sr}_{1-x}\text{Ba}_x\text{Bi}_2\text{B}_2\text{O}_7$ solid solutions were calculated. The band gaps for solid solutions were determined by the absorption spectroscopy. A similarity of thermal and compositional deformations has been established. These deformations were compared with the crystal structure of $\text{Sr}_{1-x}\text{Ba}_x\text{Bi}_2\text{B}_2\text{O}_7$ solid solutions.

Keywords: compositional deformations, borates, thermal expansion, solid solutions

DOI: 10.1134/S1087659623600990

INTRODUCTION

Recently, crystal structures with planar anionic groups $[\text{BO}_3]^{3-}$ and $[\text{B}_3\text{O}_6]^{3-}$ have attracted great interest among nonlinear optical (NLO) materials. The influence of $[\text{BO}_3]^{3-}$ and $[\text{B}_3\text{O}_6]^{3-}$ anionic groups on the NLO properties is considered in the [1–3]. Compounds containing these groups exhibit high birefringence and second harmonic generation (SHG). Many compounds containing $[\text{BO}_3]^{3-}$ and $[\text{B}_3\text{O}_6]^{3-}$ groups are transparent from visible to deep ultraviolet regions [1]. Due to the configuration of the $[\text{BO}_3]$ groups, these compounds will exhibit greater optical anisotropy between two directions parallel and perpendicular to the plane of π -conjugated $[\text{BO}_3]^{3-}$ and $[\text{B}_3\text{O}_6]^{3-}$ groups [4]. Typically, the $[\text{BO}_3]^{3-}$ and $[\text{B}_3\text{O}_6]^{3-}$ groups are arranged parallel or almost parallel to each other, and this arrangement leads to high anisotropy of thermal expansion [5].

There are structurally similar $\text{ABi}_2\text{B}_2\text{O}_7$ ($A = \text{Ca}, \text{Sr}, \text{Ba}$) borates family of prospective optical compounds, which was doped by Eu^{3+} , Tm^{3+} and Sm^{3+} [6–17]. Crystal structures of this family consist of isolated $[\text{BO}_3]^{3-}$ triangular radicals linked by MO_6 or MO_9 polyhedra into layers parallel to ab plane.

This paper reports on the absorption spectroscopy and compositional deformations of $\text{Sr}_{1-x}\text{Ba}_x\text{Bi}_2\text{B}_2\text{O}_7$ solid solutions and low-temperature powder X-ray diffraction of $\text{SrBi}_2\text{B}_2\text{O}_7$.

EXPERIMENTAL

Synthesis

The $\text{Sr}_{1-x}\text{Ba}_x\text{Bi}_2\text{B}_2\text{O}_7$ ($x = 0.00, 0.25, 0.50, 0.65, 0.75, 0.85, 1.00$) solid solutions were prepared by combining polycrystalline H_3BO_3 (Neva Reaktiv, 99.90% purity), Bi_2O_3 (Reahim, 99.99% purity) and SrCO_3 (Reahim, 99.99% purity) substituted with BaCO_3 (Reahim, 99.99% purity) in the appropriate stoichiometric ratios. The synthesis was carried out according to the procedure described in [11, 16]. The mixtures of raw materials were ground with an agate mortar and pestle for 2 h. Then the powders were pressed into pellets using a hydraulic press (LabTools) at a pressure of 80 bar. The pellets were placed on platinum crucibles and melted in the Nabertherm HTC furnace at 950°C for 30 min. The obtained melt was poured out onto a cold steel plate. Then, the polycrystalline samples were obtained by crystallization of glass ceramics at 600°C for 10 h.

Powder X-Ray Diffraction Data

Powder X-ray diffraction data for $\text{Sr}_{1-x}\text{Ba}_x\text{Bi}_2\text{B}_2\text{O}_7$ ($x = 0.00, 0.25, 0.50, 0.65, 0.75, 0.85, 1.00$) were collected using a Rigaku MiniFlex II diffractometer ($\text{CuK}\alpha$, $2\theta = 10^\circ\text{--}70^\circ$, step 0.02°). The phase composition was determined using PDXL integrated X-ray powder diffraction software and PDF-2 2016 (ICDD) database. X-ray phase analysis revealed that the poly-

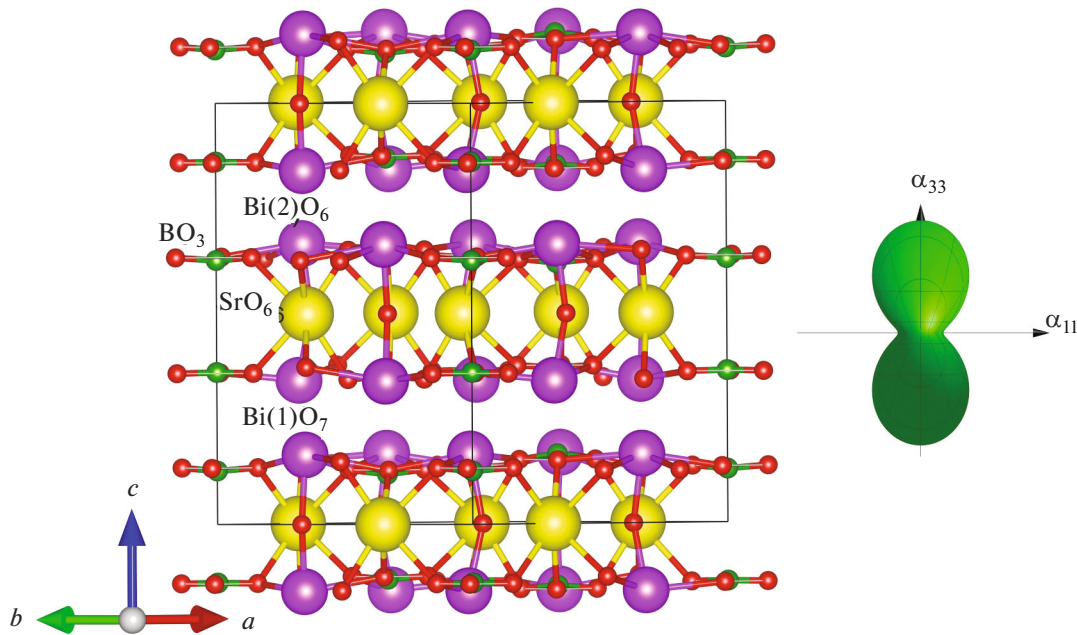


Fig. 1. Crystal structure of $\text{SrBi}_2\text{B}_2\text{O}_7$ with the figure of thermal expansion.

crystalline samples of $\text{Sr}_{1-x}\text{Ba}_x\text{Bi}_2\text{B}_2\text{O}_7$ ($x = 0.00, 0.25, 0.50, 0.65, 0.75, 0.85, 1.00$) were homogenous.

Low-Temperature X-Ray Diffraction

$\text{SrBi}_2\text{B}_2\text{O}_7$ borate was studied using the method of the low-temperature X-ray diffraction. Measurements were carried out using a Rigaku Ultima IV diffractometer ($\text{CuK}_{\alpha 1+2}$ -radiation, 40 kV, 40 mA, reflection geometry, DTEX/ULTRA detector, temperature step 25°C , average cooling rate 40°C/h). Temperature range from -175 to 25°C . Sample was prepared by precipitation from a heptane suspension on a Pt plate. The unit cell parameters were refined using the least-square method at different temperatures. The parameters temperature dependences were described by quadratic polynomials. The unit cell parameters, the experimental data processing, and the calculation of the thermal expansion coefficients were performed within the Theta to Tensor program [18].

Absorption Spectroscopy

Absorption spectra were measured on a double-beam spectrophotometer Lambda 1050 (Perkin-Elmer) equipped with a 150 mm integrating sphere, which allows to correctly measure the absorption spectra of the diffuse scattering samples.

RESULTS AND DISCUSSION

The $\text{Sr}_{1-x}\text{Ba}_x\text{Bi}_2\text{B}_2\text{O}_7$ solid solutions crystallize in the hexagonal crystal system, $P6_3$ space group. The

crystal structures of these solid solutions are similar, but the sizes of the unit cell are different: $a = 9.1404(4) \text{ \AA}$, $c = 13.0808(6) \text{ \AA}$ for $\text{SrBi}_2\text{B}_2\text{O}_7$ and $a = 5.3378(8) \text{ \AA}$, $c = 13.583(2) \text{ \AA}$ for $\text{BaBi}_2\text{B}_2\text{O}_7$. In the area of immiscibility $x \approx 0.65$ reduced cell with the parameters $a_{\text{Ba}} = a_{\text{Sr}}/\sqrt{3}$ is formed [16]. The $\text{BaBi}_2\text{B}_2\text{O}_7$ crystal structures consist of isolated BO_3 triangles and 3 sites ($M1$, $M2$ and $M3$) for large cations between them. $\text{SrBi}_2\text{B}_2\text{O}_7$ crystal structure contains six symmetrically independent BO_3 radicals with the average $\langle \text{B-O} \rangle$ bond lengths in the range $1.36\text{--}1.37 \text{ \AA}$ [15], in general agreement with the average value of 1.36 \AA given for borates [19]. The $\text{SrBi}_2\text{B}_2\text{O}_7$ crystal structure is formed by $\{\text{SrBi}_2\text{B}_2\text{O}_7\}_\infty$ layers in ab plane from BO_3 triangles, ψ -tetrahedral BiO_3 groups, and SrO_6 triangular prisms (Fig. 1). The interlayer space is $\sim 4 \text{ \AA}$ and the layers are connected by weak Bi-O bonds with a length of $2.92\text{--}2.95 \text{ \AA}$.

The unit cell parameters and volume of $\text{Sr}_{1-x}\text{Ba}_x\text{Bi}_2\text{B}_2\text{O}_7$ solid solutions increase on the substitution of Sr by Ba. The dependence of unit cell parameters on the chemical composition was approximated by a linear function: $a_x = (9.128 + 0.122x) \text{ \AA}$, $c_x = (13.053 + 0.521x) \text{ \AA}$, $V_x = (941.4 + 65.0x) \text{ \AA}^3$ [16]. It allows us to calculate the coefficients of compositional deformations: $\gamma_a = 13.37 \times 0.1 (\text{at } \%)^{-1}$, $\gamma_c = 39.91 \times 0.1 (\text{at } \%)^{-1}$, $\gamma_V = 69.05 \times 0.1 (\text{at } \%)^{-1}$.

The temperature dependencies of the $\text{SrBi}_2\text{B}_2\text{O}_7$ unit cell parameters (Fig. 2) were approximated in temperature range from -175 to 25°C by linear func-

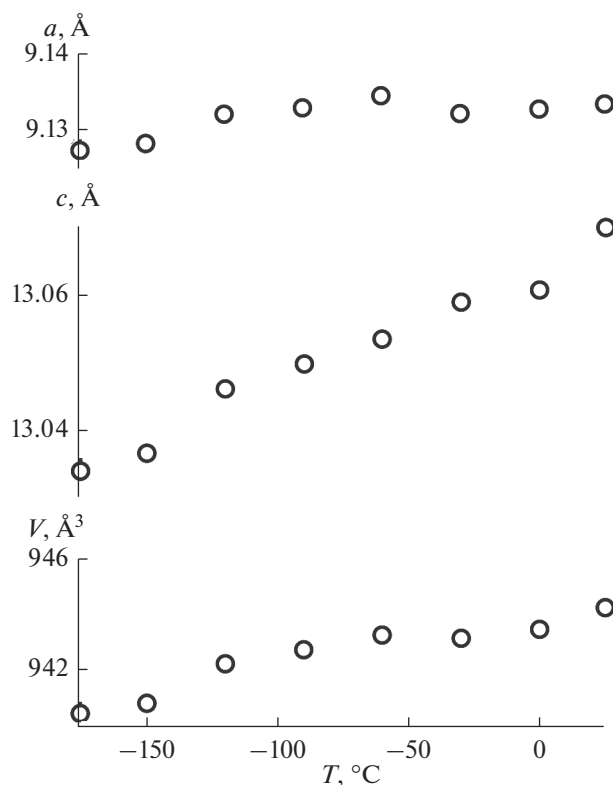


Fig. 2. Temperature dependencies of $\text{SrBi}_2\text{B}_2\text{O}_7$ unit cell parameters.

tion. The equations are as follows: $a_t = 9.1339 + 0.024 \times 10^{-3}t$, $c_t = 13.0646 + 0.168 \times 10^{-3}t$, $V_t = 943.9 + 17.1115 \times 10^{-3}t$. The main coefficients of thermal expansion are: $\alpha_a = 2.6 \times 10^{-6} \text{C}^{-1}$, $\alpha_c = 12.9 \times 10^{-6} \text{C}^{-1}$, $\alpha_V = 18.0 \times 10^{-6} \text{C}^{-1}$.

Previously, we studied the thermal expansion coefficients of these $\text{Sr}_{1-x}\text{Ba}_x\text{Bi}_2\text{B}_2\text{O}_7$ solid solutions in the temperature range 20–750°C [16]. The compositional deformations and thermal expansion lead to the similar changes of unit cell parameters and volume of solid solutions. Thus, the structures of $\text{Sr}_{1-x}\text{Ba}_x\text{Bi}_2\text{B}_2\text{O}_7$ solid solutions have similar distortions upon heating and $\text{Sr} \rightarrow \text{Ba}$ substitution. It allows us to calculate the compositional equivalents of the thermal expansion $\gamma/\alpha \text{ } ^\circ\text{C} \text{ (at \%)}^{-1}$ (Table 1).

The absorption spectra of the samples in the region of the blue edge of the transparency window are presented in Fig. 3. The absorption spectra were used to determine the band gap in the Tauc plot. The obtained band gap is the same within the error limits for all studied samples and is equal to about 3.1 eV except for sample with $x = 0.85$ (Table 2). For comparison, $\text{CaBi}_2\text{B}_4\text{O}_{10}$ has a band gap of 3.6 eV [20]. Probably, $x = 0.85$ sample has a larger number of localized states in the band gap. There is a tendency for increase of the band gap with increasing barium content.

According to [21], a certain dependence of the band gap on the ionic radius of the cation appears. As the size of the cation increases, the band gap increases. For example, for tungstates of alkaline earth metals, the band gap changes as follows: CaWO_4 (4.94 eV), SrWO_4 (5.08 eV) and BaWO_4 (5.26 eV). Accordingly, this can explain the same trend for $\text{Sr}_{1-x}\text{Ba}_x\text{Bi}_2\text{B}_2\text{O}_7$ solid solutions. Thus, the replacement of Sr with Ba, which has a larger ionic radius [22], leads to an increase in the band gap.

Since deformations of the crystal structure reveal the features of the structure, the deformations that occur under the influence of different factors are similar. One example of such a manifestation of similarity

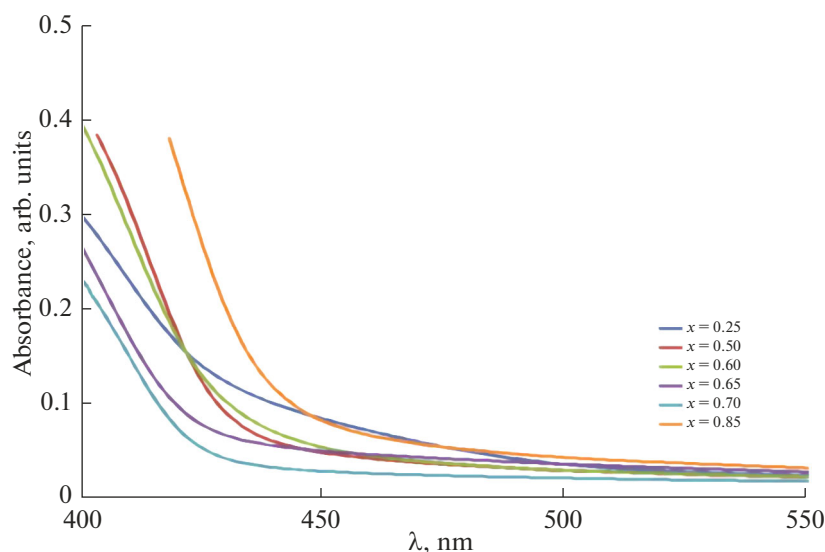


Fig. 3. Absorption spectra of $\text{Sr}_{1-x}\text{Ba}_x\text{Bi}_2\text{B}_2\text{O}_7$ solid solutions.

Table 1. Compositional equivalents of the thermal expansion γ/α °C (at %)⁻¹ for Sr_{1-x}Ba_xBi₂B₂O₇

x_{Ba}	γ/α_a	γ/α_c	γ/α_V
25°C			
0	35	17	23
0.25	52	17	25
0.50	41	18	24
0.65	34	22	27
0.70	43	19	26
1	24	20	22
325°C			
0	23	15	18
0.25	23	15	18
0.50	22	15	17
0.65	18	15	17
0.70	21	14	17
1	19	15	17
625°C			
0	17	13	15
0.25	14	12	14
0.50	16	12	14
0.65	13	12	13
0.70	14	12	13
1	16	12	14

Table 2. The blue edge of the transparency window of Sr_{1-x}Ba_xBi₂B₂O₇ samples

x	Blue edge of the transparency window, nm
0.25	414
0.50	418
0.60	417
0.65	407
0.70	404
0.85	430

is the well-known stabilization of high-temperature modification by impurities [23].

If Sr is replaced by Ba in Sr_{1-x}Ba_xBi₂B₂O₇ solid solutions, the unit cell metric changes, and if Sr is replaced by Ca, even the crystal system changes. Thus, CaBi₂B₂O₇ crystallizes in the orthorhombic system, space group *Pnma* [24] or *Pna2₁* [15]. Despite the similarity of compositional and thermal deformations, when the temperature decreases, SrBi₂B₂O₇ does not change its symmetry at least to a temperature of -175°C.

CONCLUSIONS

Thermal expansion coefficients of SrBi₂B₂O₇ borate were determined by in situ powder X-ray diffraction in the temperature range from -175 to 25°C. Compositional deformations of Sr_{1-x}Ba_xBi₂B₂O₇ solid solutions were calculated. The band gaps for solid solutions were determined by the absorption spectroscopy. A similarity of thermal and compositional deformations has been established. These deformations were compared with the crystal structure of Sr_{1-x}Ba_xBi₂B₂O₇ solid solutions. With temperature increasing and with the replacement of Sr by Ba, parameter *c* increases much more intensely than parameter *a*. It was revealed that with increasing Ba content, the band gap of solid solutions increases. This dependence is due to the fact that the ionic radius of Ba is greater than the ionic radius of Sr.

ACKNOWLEDGMENTS

The authors used the equipment of the Center of X-ray Diffraction Studies and the Center for Optical and Laser Materials Research at St. Petersburg State University.

FUNDING

The work was supported by the Russian Science Foundation (project no. 22-13-00317) (XRD experiments and calculations) and the Ministry of Science and Higher Education of the Russian Federation within the scientific tasks of the Institute of Silicate Chemistry, Russian Academy of Sciences (project no. 0081-2022-0002) (compositional deformations calculation).

CONFLICT OF INTEREST

The authors of this work declare that they have no conflicts of interest.

REFERENCES

- Gong P., Liu, X., Kang, L., and Lin, Z., Inorganic planar π -conjugated groups in nonlinear optical crystals: Review and outlook, *Inorg. Chem. Front.*, 2020, vol. 7, no. 4, pp. 839–852. <https://doi.org/10.1039/C9QI01589B>
- Shen, Y., Zhao, S., and Luo, J., The role of cations in second-order nonlinear optical materials based on π -conjugated [BO₃]³⁻ groups, *Coord. Chem. Rev.*, 2018, vol. 366, pp. 1–28. <https://doi.org/10.1016/j.ccr.2018.03.012>
- Mutailipu, M., Poeppelmeier, K.R., and Pan, S., Borates, A rich source for optical materials, *Chem. Rev.*, 2021, vol. 121, no. 3, pp. 1130–1202. <https://doi.org/10.1021/acs.chemrev.0c00796>
- Chen, C., Sasaki, T., Li, R., Wu, Y., Lin, Z., Mori, Y., Hu, Z., Wang, J., Uda S., Yoshimura M., and Kaneda, Y., *Nonlinear Optical Borate Crystals*, Weinheim: Wiley-VCH, 2012.

5. Bubnova, R.S. and Filatov, S.K., Self-assembly and high anisotropy thermal expansion of compounds consisting of TO_3 triangular radicals, *Struct. Chem.*, 2016, vol. 27, no. 6, pp. 1647–1662.
<https://doi.org/10.1007/s11224-016-0807-9>
6. Li, J., Yan, H., and Yan, F., Luminescence properties of a novel orange-red $\text{CaBi}_2\text{B}_2\text{O}_7:\text{Eu}^{3+}$ phosphor for near-UV pumped W-LEDs, *Optik*, 2016, vol. 127, no. 10, pp. 4541–4544.
<https://doi.org/10.1016/j.ijleo.2016.01.155>
7. Li, J., Yan, H., and Yan, F., A novel high color purity blue-emitting phosphor: $\text{CaBi}_2\text{B}_2\text{O}_7:\text{Tm}^{3+}$, *Mater. Sci. Eng., B*, 2016, vol. 209, pp. 56–59.
<https://doi.org/10.1016/j.mseb.2016.03.004>
8. Li, Z., Pian, Q., Li, L., Sun, Y., and Zheng, S., Luminescence properties of $\text{SrBi}_2\text{B}_2\text{O}_7:\text{Eu}^{3+}$ orange-red phosphor, *Optik*, 2018, vol. 161, pp. 38–43.
<https://doi.org/10.1016/j.ijleo.2018.01.132>
9. Wu, L., Bai, Y., Wu, L., Yi, H., Kong, Y., Zhang, Y., and Xu, J., Sm^{3+} and Eu^{3+} codoped $\text{SrBi}_2\text{B}_2\text{O}_7$: A red-emitting phosphor with improved thermal stability, *RSC Adv.*, 2017, vol. 7, pp. 1146–1153.
<https://doi.org/10.1039/c6ra26752a>
10. Majhi, K. and Varma, K.B.R., Structural, dielectric and optical properties of transparent glasses and glass-ceramics of $\text{SrBi}_2\text{B}_2\text{O}_7$, *J. Non-Cryst. Solids*, 2008, vol. 354, pp. 4543–4549.
<https://doi.org/10.1016/j.jnoncrysol.2008.06.010>
11. Shablinskii, A.P., Drozdova, I.A., Volkov, S.N., Krzhizhanovskaya, M.G., and Bubnova R.S., Production and study of glass ceramics in $\text{Sr}_{1-x}\text{Ba}_x\text{Bi}_2\text{B}_2\text{O}_7$ system, *Fiz. Khim. Stekla*, 2012, vol. 38, no. S6, pp. 886–889.
12. Singh, V.P., Kushwaha, H.S., and Vaish, R. Photocatalytic study on $\text{SrBi}_2\text{B}_2\text{O}_7$ ($\text{SrO}-\text{Bi}_2\text{O}_3-\text{B}_2\text{O}_3$) transparent glass ceramics, *Mater. Res. Bull.*, 2018, vol. 99, pp. 453–459.
<https://doi.org/10.1016/j.materresbull.2017.11.043>
13. Shablinskii, A.P., Povolotskii, A.V., Drozdova, I.A., Kolesnikov, I.E., and Bubnova, R.S., New luminescent $\text{BaBi}_{2-x}\text{Eu}_x\text{B}_2\text{O}_7$ glassmaterials, *Glass Phys. Chem.*, 2019, vol. 45, no. 1, pp. 74–78.
<https://doi.org/10.1134/S1087659619010097>
14. Padmaja, G., Devarajulu, G., Raju, B.D.P., Turpu, G.R., Srishailam, K., Reddy, B.V., and Kumar, G.P., Synthesis of $\text{Sr}_{1-x}\text{Ba}_x\text{Bi}_2\text{B}_2\text{O}_7$ glass ceramics: A study for structure and characterization using experimental techniques and DFT method, *J. Mol. Struct.*, 2020, vol. 1220, p. 128660.
<https://doi.org/10.1016/j.molstruc.2020.128660>
15. Barbier, J. and Cranswick, L.M.D., The non-centrosymmetric borate oxides, $\text{MBi}_2\text{B}_2\text{O}_7$ ($M = \text{Ca}, \text{Sr}$), *J. Solid State Chem.*, 2006, vol. 179, no. 12, pp. 3958–3964.
<https://doi.org/10.1016/j.jssc.2006.08.037>
16. Bubnova R.S., Shablinskii, A.P., Volkov, S.N., Filatov, S.K., Krzhizhanovskaya, M.G., and Ugolkov, V.L., Crystal structures and thermal expansion of $\text{Sr}_{1-x}\text{Ba}_x\text{Bi}_2\text{B}_2\text{O}_7$ solid solutions, *Glass Phys. Chem.*, 2016, vol. 42, pp. 337–348.
<https://doi.org/10.1134/S1087659616040040>
17. Shablinskii, A.P., Povolotskiy, A.V., Kolesnikov, I.E., Biryukov, Y.P., Bubnova, R.S., Avdontceva, M.S., Demina, S.V., and Filatov, S.K., Novel red-emitting color-tunable phosphors $\text{BaBi}_{2-x}\text{Eu}_x\text{B}_2\text{O}_7$ ($x = 0-0.40$): Study of the crystal structure and luminescence. *J. Solid State Chem.*, 2022, vol. 307, p. 122837.
<https://doi.org/10.1016/j.jssc.2021.122837>
18. Bubnova, R.S., Firsova, V.A., and Filatov, S.K., Software for determining the thermal expansion tensor and the graphic representation of its characteristic surface (theta to tensor-TTT), *Glass Phys. Chem.*, 2013, vol. 39, no. 3, pp. 347–360.
<https://doi.org/10.1134/S108765961303005X>
19. Bubnova R.S. and Filatov, S.K., High-temperature borate crystal chemistry, *Z. Kristallogr.—Cryst. Mater.*, 2013, vol. 228, no. 9, pp. 395–428.
<https://doi.org/10.1524/zkri.2013.1646>
20. Shablinskii, A.P., Povolotskiy, A.V., Yuriev, A.A., Bubnova, R.S., Kolesnikov, I.E., and Filatov, S.K., Novel $\text{CaBi}_2\text{B}_4\text{O}_{10}:\text{Eu}^{3+}$ red phosphor: Synthesis, crystal structure, luminescence and thermal expansion, *Solid State Sci.*, 2020, vol. 106, p. 106280.
<https://doi.org/10.1016/j.solidstatesciences.2020.106280>
21. Lacomba-Perales, R., Ruiz-Fuertes, J., Errandonea, D., Martínez-García, D., and Segura A., Optical absorption of divalent metal tungstates: Correlation between the band-gap energy and the cation ionic radius, *Europhys. Lett.*, 2008, vol. 83, no. 3, p. 37002.
<https://doi.org/10.1209/0295-5075/83/37002>
22. Shannon, R.D., Revised effective ionic radii and systematic studies of interatomic distances in halides and chalcogenides, *Acta Crystallogr.*, 1976, vol. A32, pp. 751–767.
<https://doi.org/10.1107/S0567739476001551>
23. Filatov, S.K., *Vysokotemperaturnaya kristalloghimiya. Teoriya, metody i resul'taty issledovaniy* (High Temperature Crystal Chemistry: Theory, Methods and Results of Studies), Leningrad: Nedra, 1990.
24. Volkov, S.N., Bubnova, R.S., Shorets, O.U., Ugolkov, V.L., and Filatov, S.K., Crystal structure and strong uniaxial negative thermal expansion of $\text{CaBi}_2\text{B}_2\text{O}_7$ borate, *Inorg. Chem. Commun.*, 2020, vol. 122, p. 108262.
<https://doi.org/10.1016/j.inoche.2020.108262>

Publisher's Note. Pleiades Publishing remains neutral with regard to jurisdictional claims in published maps and institutional affiliations.